Cancer Science
Japanese Cancer Association JCA
Open Access

Myeloid heme oxygenase-1 promotes metastatic tumor colonization in mice

Heng-Huei Lin, Ming-Tsai Chiang, Po-Chiao Chang and Lee-Young Chau

Institute of Biomedical Sciences, Academia Sinica, Taipei, Taiwan, China

Key words
Cancer, colonization, heme oxygenase-1, metastasis, myeloid cells

Correspondence
Lee-Young Chau, Institute of Biomedical Sciences, Academia Sinica, Nankang, Taipei 115, Taiwan.
Tel: 886-2-2652-3931; Fax: 886-2-2785-8847;
E-mail: lyc@ibms.sinica.edu.tw

Funding Information
This work was supported in part by the funding from the Academia Sinica and by a grant From the National Science Council of Taiwan (NSC 100-2320-B-001-010-MY3).

Received September 16, 2014; Revised December 29, 2014; Accepted January 5, 2015

Cancer Sci **106** (2015) 299–306

doi: 10.1111/cas.12604

Heme oxygenase-1 (HO-1) is a heme degradation enzyme with antioxidant and immune-modulatory functions. HO-1 promotes tumorigenesis by enhancing tumor cell proliferation and invasion. Whether HO-1 has an effect on cancer progression through stromal compartments is less clear. Here we show that the growth of tumor engrafted subcutaneously in syngeneic mice was not affected by host HO-1 expression. However, lung metastasis arisen from subcutaneous tumor or circulating tumor cells was significantly reduced in HO-1$^{+/-}$ mice comparing to wild type (WT) mice. The reduced lung metastasis was also observed in B6 mice bearing HO-1$^{+/-}$ bone marrow as comparing to WT chimeras, indicating that HO-1 expression in hematopoietic cells impacts tumor colonization at the metastatic site. Further experiments demonstrated that the numbers of myeloid cells recruited to pulmonary premetastatic niches and metastatic loci were significantly lower in HO-1$^{+/-}$ mice than in WT mice. Likewise, the extents of tumor cell extravasation and colonization at the metastatic loci in the early phase of metastasis were significantly lower in HO-1$^{+/-}$ mice. Mechanistic studies revealed that HO-1 impacted chemoattractant-induced myeloid cell migration by modulating p38 kinase signaling. Moreover, myeloid HO-1-induced expressions of vascular endothelial growth factor and interleukin-10 promoted tumor cell transendothelial migration and STAT3 activation *in vitro*. These data support a pathological role of myeloid HO-1 in metastasis and suggest a possibility of targeting myeloid HO-1 for cancer treatment.

Myeloid cells have been shown to influence cancer initiation and progression in many ways.[1] The tumor-associated macrophages produce angiogenic and growth factors and the matrix metalloproteases to promote tumor cell growth, angiogenesis and metastasis.[1,2] These cells also induce immune suppression by producing immunosuppressive cytokines, such as interleukin-10 (IL-10) and transforming growth factor-beta. Moreover, the accumulation of myeloid-derived suppressor cells (MDSC) in the tumor microenvironment exerts a profound effect on tumor progression through their potent immunosuppressive activity on T cells.[3] In addition to their multiple roles in primary tumors, increasing evidence has revealed the involvement of myeloid cells in supporting seeding, engraftment and survival of metastatic tumor cells in distant sites.[1,2,4] Studies have shown that soluble factors secreted by the primary tumor can prime distant organs by inducing the expressions of fibronectin and chemoattractants in focal areas, which subsequently promotes the recruitment of myeloid cells to form a receptive pre-metastatic niche for disseminating tumor cell invasion and growth.[5–8] Moreover, a population of inflammatory monocytes/macrophages can be recruited to the metastatic sites early in the metastasis process to facilitate the seeding and survival of tumor cells.[9,10] These findings highlight the pivotal role of myeloid cells in cancer metastasis. Increasing our understanding of the intrinsic factor(s) that modulate the prometastatic function of myeloid cells could pave the way for new therapeutics for metastatic disease.

Heme oxygenase-1 (HO-1) is a rate-limiting enzyme catalyzing the oxidative degradation of heme to release free iron, carbon monoxide (CO) and biliverdin.[11] In addition to its primary role in heme catabolism, HO-1 also participates in various pathophysiological conditions, including cancer. HO-1 is highly induced in various types of cancers.[12] HO-1 immunoreactivity was detected in both tumor and stromal cells of cancer tissues, including tumor-associated macrophages.[13–17] HO-1 promotes cancer cell proliferation and survival.[18] Whether HO-1 expression in stromal cells impacts cancer progression is less clear. Over the past decade, considerable evidence has revealed the profound effects of HO-1 on myeloid cells.[11] HO-1 and its reaction byproduct, CO, suppress the expression of proinflammatory genes, such as tumor necrosis factor alpha, but augment the expression of immunosuppressive IL-10 in macrophages.[19] HO-1/CO also promotes inflammation-associated angiogenesis through upregulating vascular endothelial growth factor (VEGF) expression.[20] Furthermore, HO-1 mediates MDSC-induced suppression of alloreactive T cells.[21] We postulated that HO-1 may influence cancer progression through modulating myeloid cells. In the present study we performed the syngeneic tumor graft experiments with wild type (WT) and HO-1 $^{+/-}$ mice, and found that the lung metastasis arising from primary tumor or circulating tumor cells was much more prominent in WT mice. Likewise, more lung nodules were developed in chimeric B6 mice bearing WT-BM than HO-1$^{+/-}$ chimeras, supporting the involvement of hematopoietic HO-1 in this process. We

performed additional experiments to disclose the molecular and cellular mechanisms involved.

Materials and Methods

Tumor cell culture. Lewis lung carcinoma (LLC) and B16F10 melanoma cells were cultured in DMEM supplemented with 10% FBS. GFP-expressing LLC cells were established by infection with lentivirus bearing the GFP gene and selected with 4 μg/mL puromycin. To label B16F10 cells with fluorescent dye, cells were incubated with 10 μM CellTracker Orange CMTMR (5-(and-6)-(((4-Chloromethyl)Benzoyl)Amino)Tetramethylrhodamine) (Invitrogen, Carlsbad, CA, USA) or CellTracker Green CMFDA (5-Chloromethylfluorescein Diacetate) (Invitrogen) in serum-free DMEM at 37°C for 1 h, followed by incubation in complete medium for another 30 min. After 3 PBS washes, cells were trypsinized and used for subsequent experiments immediately.

Bone marrow-derived macrophages. Bone marrow (BM) cells were removed from the femurs and tibias of mice and the induction of macrophage differentiation was performed as described.[22]

Preparation of conditional medium. Lewis lung carcinoma and B16F10 cells (3×10^6) plated in a 10-cm petri dish or 5×10^5 bone marrow-derived macrophages (BMDM) plated in a 3.5-cm dish were cultured in serum-free DMEM (phenol red free) containing 1% BSA for 18 h. Medium were collected, passed through a 0.22-μm filter, and stored as aliquots at −80°C prior to use.

Animal experiments. The animal experimental procedures were approved by the Institutional Animal Care and Utilization Committee of the Academia Sinica, Taiwan. WT and HO-$1^{+/-}$ mice, originally on B6/129SV mixed background, were backcrossed 10 generations onto the C57BL/6J genetic background. To generate B6 chimeric mice reconstituted with WT or HO-$1^{+/-}$ BM, we performed BM transplantation with lethally irradiated C57BL/6J mice (6-week-old male) as described previously.[23] To examine the spontaneous lung metastasis, we injected 2×10^6 LLC cells subcutaneously into the right flanks of mice (8–10-week-old male) for 3 weeks. The subcutaneous primary tumors and lungs were removed for further assessments. To perform the experimental lung metastasis, GFP-labeled LLC cells (1×10^5) or B16F10 cells (2×10^5) were injected i.v. via tail veins of animals. Mice were sacrificed at indicated times and lung tissues were examined. To assess premetastatic niche formation, mice received i.p. injection of control medium or tumor cell-conditional medium (CM) (300 μL/mouse) for 10 consecutive days prior to sacrifice. In some experiments, mice received an i.v. injection of fluorescent dye-labeled B16F10 cells for indicated times. The lung tumor metastases were examined using a fluorescent stereomicroscope (STEREO Lumar V12; Carl Zeiss, Munich, Germany), and quantified by MetaMorph software, Molecular Devices, Sunnyvale, CA, USA.

Real time quantitative PCR. RNA isolation, reverse transcription reaction and real-time PCR were performed as described previously.[23] The primer pairs used are summarized in Table S1.

Transwell migration assay. Mouse splenic $CD11b^+$ cells were isolated using the EasySep mouse CD11b positive selection kit (Stemcell Tech, Vancouver, BC, Canada). Cell migration was assessed using 24-well Transwell plates as described previously.[24]

Immunohistochemistry and immunofluorescence staining. Paraffin-embedded sections were blocked with 5% normal goat serum, followed by incubation with rat anti-mouse CD11b (eBioscience San Diego, CA, USA) for 1 h at 37°C. After 3 PBS washes, the antigen–antibody complex was detected by incubation with horseradish peroxidase-conjugated anti-rat IgG and stained with diaminobenzidine. For immunofluorescence staining, lung cryosections were blocked with 5% normal goat serum, followed by incubation with rat anti-mouse CD11b (eBioscience) or rabbit anti-mouse F4/80 antibody at 37°C for 1 h. After 3 PBS washes, sections were incubated with Alexa Fluor 555-conjugated goat anti-rat (Cell signaling Technology, Danvers, MA, USA) or Alexa Fluor 488-conjugated goat anti-rabbit (Molecular Probes, Saint Aubin, France) antibody for another 1 h at room temperature in the dark. Nuclei were then stained with DAPI and sections examined by fluorescence microscope (BX51; Olympus, Tokyo, Japan) at 200× magnification.

Confocal microscopy. Lung cryosections blocked with 5% goat serum were incubated with rat anti-CD11b and rabbit anti-phospho-STAT3 (Cell Signaling) at 37°C for 1 h. After 3 PBS washes, sections were incubated with Alexa Fluor 647-conjugated goat anti-rat (Cell Signaling) and Alexa Fluor 488-conjugated goat anti-rabbit antibodies (Molecular Probes, Saint Aubin, France) for another 1 h at room temperature in the dark. Nuclei were stained with DAPI and examined by confocol microscope (LSM 510 META; Carl Zeiss, Jena, Germany) at 400× magnification.

***In vivo* tumor cell extravasation.** 1×10^6 CMFDA-labeled B16F10 cells were injected i.v. into mice for 4 h. Lungs were fixed by perfusion with PBS containing 4% paraformaldehyde and 0.3% Triton X-100 for 15 min and then washed by PBS containing 0.1% Triton X-100. Lungs cut in small pieces were incubated with Isolectin IB4 Alexa Fluor 647 conjugates (1:50; Invitrogen) at 4°C for 24 h. After 3 PBS washes, tissues were treated with FocusClear (CelExplorer, Hsinchu, Taiwan) for an additional 24 h prior to scanning with a confocal microscope (Ultra View ERS-3FE). Images from at least eight different fields per lung were taken, and the 3-D reconstitution was performed using Velocity (Perkin Elmer, Waltham, MA, USA).

Tumor transendothelial migration assay. The transwell with pore size of 8 μm (Corning, Union city, CA, USA) was coated with 125 μg/mL Matrigel, followed by seeding with 5×10^4 SV40 transformed mouse lymph node endothelial cells (SVEC). After 42 h in culture, 1×10^5 CMFDA-labeled B16F10 cells were added onto the SVEC monolayer of the upper chamber. The lower chamber was filled with WT and HO-$1^{+/-}$ BMDM-CM alone or containing indicated amounts of goat control IgG or goat anti-VEGF antibody as indicated. After 8 h of incubation at 37°C, B16F10 cells migrated to the lower surface of the transwell membrane were fixed with 4% paraformaldehyde and examined by fluorescence microscopy. The photos from five different fields (×100 magnification) of each transwell were taken and cells counted and data presented as cell number per field.

Western blot analysis. Western blot analysis was performed as described previously.[23] The primary antibodies used were: anti-phospho-p38, anti-p38, anti-phospho-STAT3 and anti-STAT3 (all from Cell Signaling).

Statistical analysis. Results were expressed as the means ± SE. Differences between groups were examined for statistical significance using Student's *t*-test or ANOVA. A *P*-value <0.05 was considered statistically significant.

Results

Hematopoietic heme oxygenase-1 promotes lung metastasis. When the syngeneic WT and HO-$1^{+/-}$ mice received

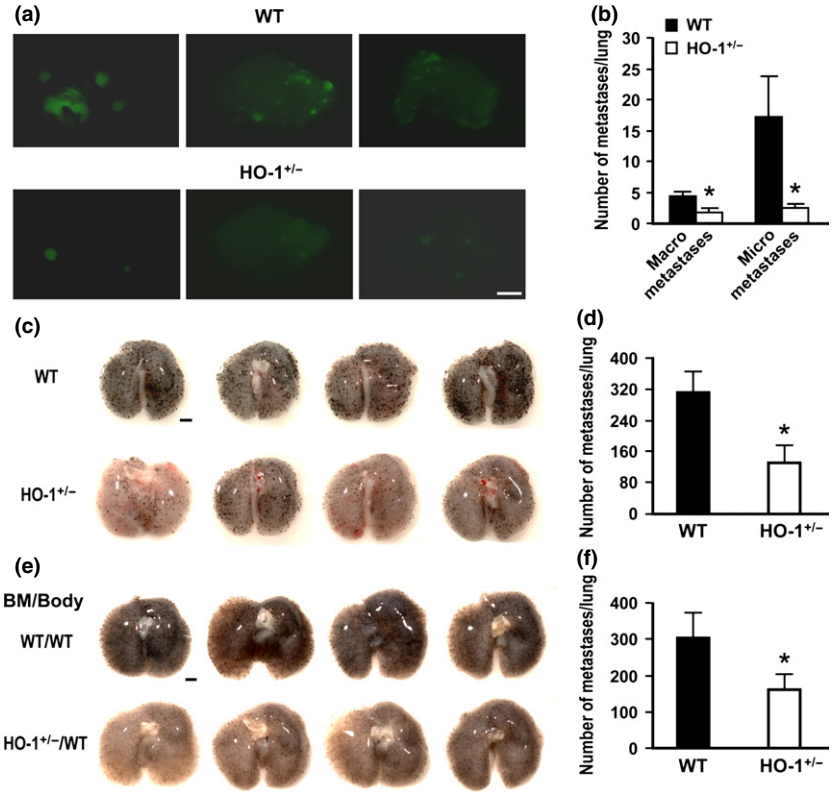

Fig. 1. Hematopoietic heme oxygenase-1 (HO-1) promotes metastasis. (a,b) Wild type (WT) and HO-1$^{+/-}$ mice (n = 8/group) received an i.v. injection of 1 × 10^5 GFP-labeled LLC cells for 2 weeks. Lungs were harvested and tumor metastases examined by fluorescence stereomicroscope. (a) The representative images. Bar = 1 mm. (b) The lung macrometastases (>1 mm^3) and micrometastases (<1 mm^3) were quantified. (c,d) WT and HO-1$^{+/-}$ mice (n = 4/group) received an i.v. injection of 2.5 × 10^5 B16F10 cells for 10 days. Lungs were harvested and tumor metastases examined (c) and quantified (d). Bar = 2 mm. (e,f) Chimeric B6 mice transplanted with WT or HO-1$^{+/-}$ bone marrow (BM) received an i.v. injection of B16F10 cells as described above. The formation of lung metastases was examined (e) and quantified (f). *P < 0.01 versus WT group.

subcutaneous injection of LLC cells in the dorsal right flanks for 3 weeks, the subcutaneous tumors grown in WT and HO-1$^{+/-}$ mice were not significantly different (Fig. S1a,b). However, examination of the lung sections revealed more metastases developed in WT mice than HO-1$^{+/-}$ counterparts (Fig. S1c,d). We then performed the experimental lung metastasis assay by directly injecting GFP-LLC cells through tail veins of mice. As shown in Figure 1(a,b), lung metastasis at 2 weeks after LLC inoculation was significantly greater in WT mice than HO-1$^{+/-}$ mice. Similar results were obtained when an experiment was performed with B16F10 cells (Fig. 1c,d). To further examine whether hematopoietic HO-1 expression impacts lung metastasis, we conducted the same experiment using chimeric B6 mice reconstituted with WT or HO-1$^{+/-}$ BM. As shown in Figure 1(e,f), the lung metastases developed at 10 days post-B16F10 inoculation were significantly lower in HO-1$^{+/-}$ chimeras compared to WT chimeras, supporting the involvement of hematopoietic HO-1 in facilitating tumor colonization at metastatic sites.

Myeloid heme oxygenase-1 influences premetastatic niches formation. To examine whether host HO-1 has an influence on the establishment of a premetastatic niche in distant organ induced by tumor-derived soluble factors,[5–8] we subjected WT and HO-1$^{+/-}$ mice to i.p. injection of CM collected from tumor cells for 10 consecutive days as reported previously.[5] The accumulation of CD11b$^+$-myeloid cells in the lung parenchyma was then examined by immunofluorescence staining. As illustrated in Figure 2(a,b), both LLC- and B16F10-CM induced substantial myeloid cell infiltration in the lungs, which was more prominent in WT mice. Flow cytometric analysis of these recruited cells demonstrated that a significant cell population expressed both CD11b and Gr-1 (Fig. S2a,b), which are the characteristic markers of MDSC. To investigate whether the accumulation of myeloid cells augments the lung metastasis of tumor cells, both WT and HO-1$^{+/-}$ mice were pretreated with B16F10-CM for 10 days, followed by i.v. injection of B16F10 cells. Results showed that lung metastasis was significantly facilitated with more tumor nodules found in the WT group (Fig. 2c,d). Immunohistochemistry again revealed more CD11b$^+$ myeloid cells clustered around B16F10 cells in the lungs of WT mice (Fig. 2e).

Heme oxygenase-1 influences tumor cell extravasation and STAT3 activation in metastatic sites. Myeloid cells, particularly inflammatory monocytes/macrophages, have been shown to promote tumor cell extravasation and survival during the early phase of metastasis.[9,10] To assess the potential impact of myeloid HO-1 on these processes, we first examined the mobilization of monocytes/macrophages to lungs of WT and HO-1$^{+/-}$ mice after i.v. injection of CMTMR-labeled B16F10 cells. As demonstrated in Figure 3(a,b), equivalent numbers of tumor cells were found in the lungs of WT and HO-1$^{+/-}$ mice at 4 h after B16F10 cell inoculation. After 24 h, tumor cells remaining in the lungs were significantly reduced. Nevertheless, more tumor cells were detected in the lungs of WT mice

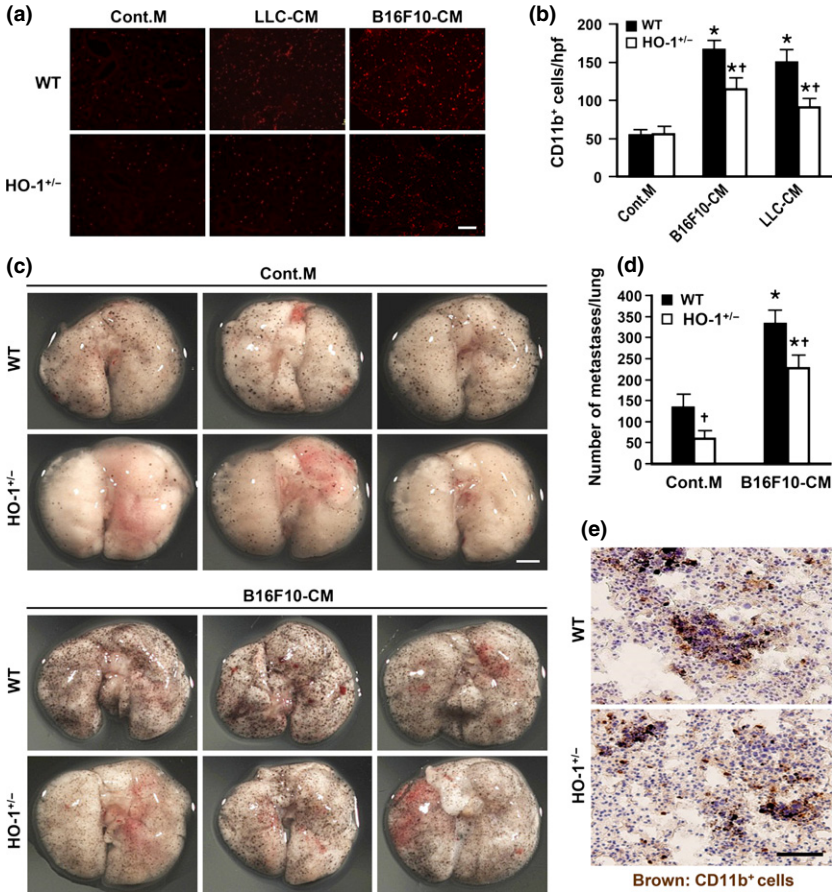

Fig. 2. Heme oxygenase-1 (HO-1) affects premetastatic niche formation. (a,b) Wild type (WT) and HO-1$^{+/-}$ mice (n = 4/group) received an i.p. injection of control medium (Cont.M) or indicated tumor cell-CM for 10 consecutive days. Lung tissues were collected for further analysis. (a) Representative images of immunofluorescence staining for CD11b^{+} cells. Bar = 200 μm. (b) Quantitative results of CD11b^{+} cells in the lungs of various treated groups. (c–e) WT and HO-1$^{+/-}$ mice received an i.p. injection of cont.M or B16F10-CM for 10 days, followed by an i.v. injection of 1×10^{6} B16F10 cells for 7 days. Lungs were harvested and formation of metastases examined (c) and quantified (d). Bar = 2 mm. (e) The representative images of immunostains for CD11b^{+} cells in the lung sections of B16F10-CM-treated WT and HO-1$^{+/-}$ mice. Bar = 100 μm. *P < 0.01 versus cont.M-treated group of same genotype; $^{\dagger}P$ < 0.01 versus WT group of same treatment. CM, conditional medium; LCC, Lewis lung carcinoma.

compared to HO-1$^{+/-}$ mice. An immunostaining experiment revealed the recruitment of significant numbers of F4/80^{+} macrophages to lungs of mice at 4 h post-B16F10 cell injection (Fig. 3a,c). Notably, the macrophage infiltration was more prominent in WT mice. Although macrophages declined at a later time point (24 h), they remained higher in the WT mice than in their HO-1$^{+/-}$ counterparts. To examine whether tumor cell extravasation is correlated with macrophage infiltration, the lungs of mice subjected to infusion of CMFDA-labeled B16F10 cells for 4 h were incubated with red fluorescent dye-conjugated isolectin B4 to stain the vasculature, followed by examination with 3-D confocal microscopy. It was shown that significant percentages of B16F10 cells were present within the blood vessels in both groups of mice (Fig. 4a,b). Nevertheless, the number of tumor cells located in the extravascular areas was much higher in WT mice compared to HO-1$^{+/-}$ mice ($14.56 \pm 1.26\%$ *vs* $10.01 \pm 1.51\%$, $P = 0.019$) at this early time point.

STAT3 signaling activated by many growth factors and cytokines is crucial for cancer cell survival and proliferation.[25] To assess whether macrophages recruited to the metastatic foci can promote tumor cell survival by activating STAT3 signaling, we performed confocal immunofluorescence with lung sections of mice receiving B16F10 cell infusion for 48 h. As illustrated in Figure 4(c), the positive immunostain for phospho-STAT3 was most prominent in tumor cells arrested in the lungs of WT mice compared to these in HO-1$^{+/-}$ mice. Moreover, the percentage of tumor cells with positive stain of phospho-STAT3 was much higher in WT mice (Fig. 4d).

Heme oxygenase-1 affects migration response of myeloid cells. To understand the molecular basis of how more myeloid cells were recruited to lungs of WT mice following tumor-CM treatment, we first examined the expressions of pulmonary genes involved in the recruitment of myeloid cells. Consistent with previous reports,[5–7] the pulmonary expressions of fibronectin, lysyl oxidase and chemoattractants, S100A8 and S100A9, were significantly increased in mice treated with tumor-CM (Fig. S3). However, the extents of induction were comparable between WT and HO-1$^{+/-}$ mice. We then examined whether HO-1 influences the migration responses of myeloid cells toward chemoattractants, particularly S100A8/S100A9, which are the major chemoattractants mediating myeloid recruitment via p38 kinase signaling.[6] As shown in Figure S4(a), HO-1 protein expression in splenic CD11b^{+} cells isolated from WT mice was much higher than that of CD11b^{+} cells from HO-1$^{+/-}$ mice. Likewise, WT-CD11b^{+} cells exhibited greater

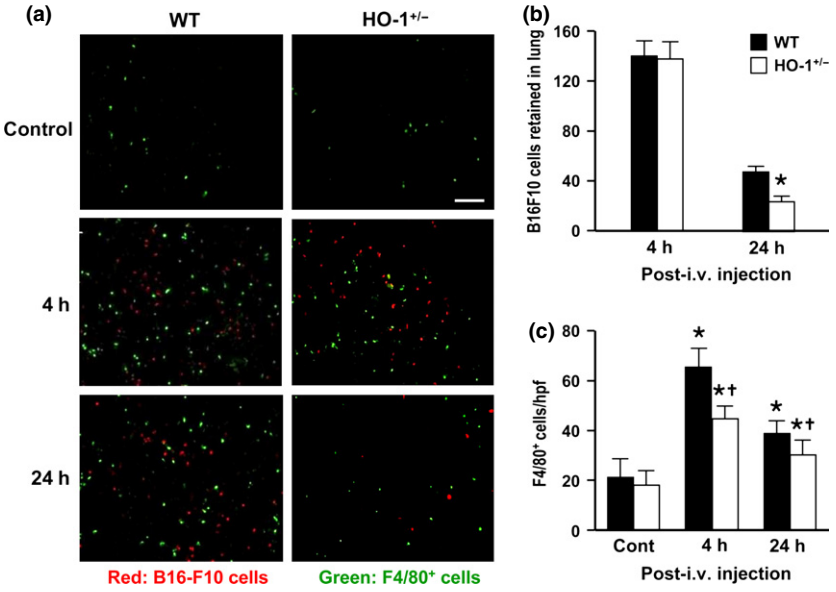

Fig. 3. Heme oxygenase-1 (HO-1) influences monocyte/macrophage mobilization to metastatic site. Wild type (WT) and HO-1$^{+/-}$ mice (n = 5/group) received an i.v. injection of PBS (control) or 1 × 10^6 CMTMR-labeled B16F10 cells. After 4 and 24 h, lungs were harvested and tissue sections were subjected to immunofluorescence staining with F4/80 antibody. (a) Representative images showing B16F10 cells (red) and F4/80$^+$ macrophages (green) in the lungs of treated mice. Bar = 100 μm. (b) Quantitative results of B16F10 cells in various groups. *P < 0.01 versus WT group. (c) Quantitative results of F4/80$^+$ macrophages in various groups. *P < 0.01 versus control group of same genotype; $^{\dagger}P$ < 0.03 versus WT group.

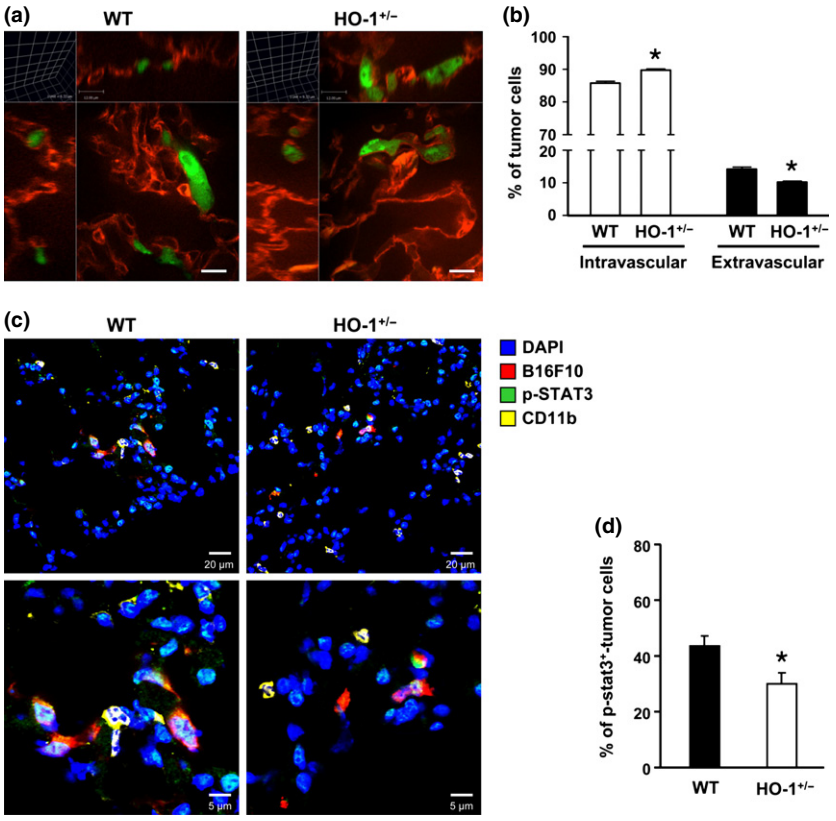

Fig. 4. Heme oxygenase-1 (HO-1) influences extravasation and STAT3 activation of metastatic tumor cells. (a,b) Wild type (WT) and HO-1$^{+/-}$ mice (n = 5/group) received an i.v. injection of 1 × 10^6 CMFDA-labeled B16F10 cells for 4 h. Pulmonary vasculature was labeled by isolectin IB4 Alexa Fluor 647 conjugates. (a) Representative 3-D confocal images of lungs. Bar = 12 μm. (b) The percentages of intravascular and extravascular tumor cells were determined. *P < 0.02 versus WT group. (c) WT and HO-1$^{+/-}$ mice received an i.v. injection of 1 × 10^6 CMTMR-labeled B16F10 cells for 48 h. The lung sections were subjected to immunofluorescence staining with antibodies against p-STAT3 and CD11b, respectively. Data shown is the representative image. (d) The percentage of B16F10 cells with positive p-STAT3 immunostain in each group of mice (n = 3/group) was determined. *P < 0.02 versus WT group.

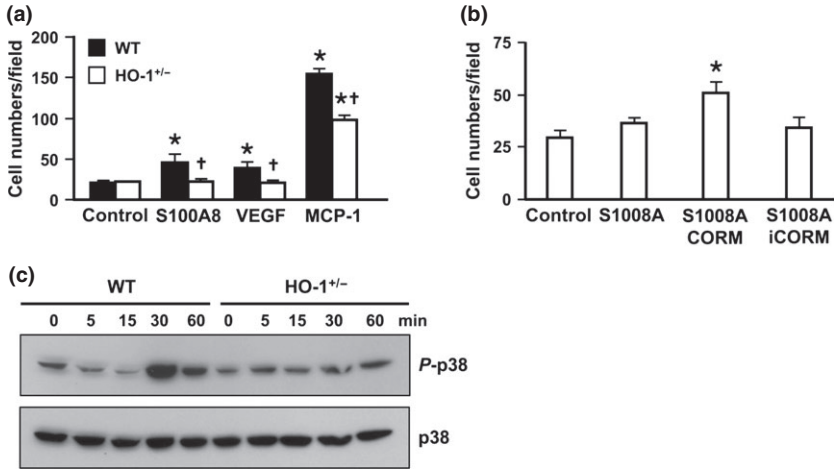

Fig. 5. Heme oxygenase-1 (HO-1) impacts chemoattractant-induced migration of myeloid cells. (a) Migration responses of wild type (WT) and HO-1$^{+/-}$ CD11b^{+} cells toward S100A8 (10 pg/mL), vascular endothelial growth factor (VEGF) (10 ng/mL), or monocyte chemoattractant protein-1 (MCP-1) (10 ng/mL). Data are mean ± SE of three independent experiments. *$P < 0.05$ versus control group of same genotype; †$P < 0.05$ versus WT group. (b) Migration response of HO-1$^{+/-}$ CD11b^{+} cells toward S100A8 in the absence or presence of 10 μM of CORM-2 or inactive CORM-2 (iCORM-2). Data are mean ± SE of three independent experiments. *$P < 0.05$ versus control. (c) WT and HO-1$^{+/-}$ bone marrow-derived macrophages were treated with 10 pg/mL of S100A8 for indicated times. The levels of phospho-p38 and total p38 examined by western blot analysis.

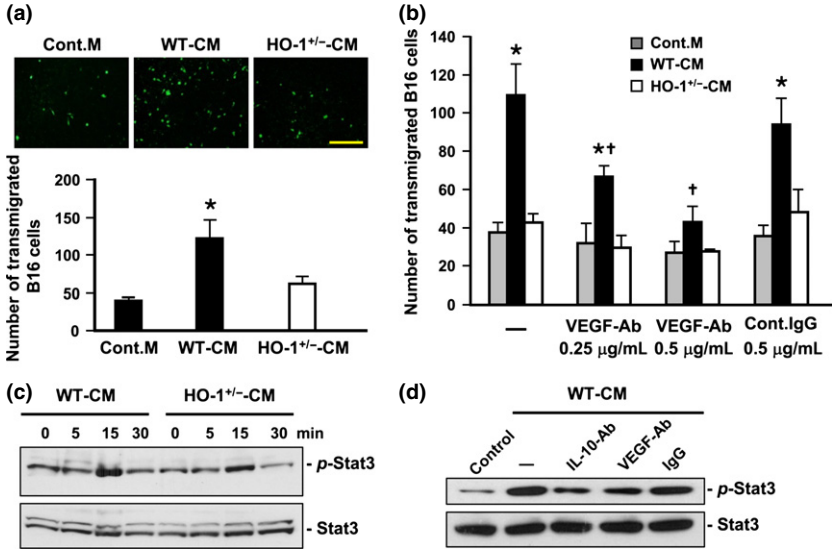

Fig. 6. Myeloid heme oxygenase-1 (HO-1)-induced vascular endothelial growth factor (VEGF) and interleukin-10 (IL-10) promote transendothelial migration and STAT3 activation of tumor cells. (a) Representative micrograph of CMFDA labeled-B16F10 cells transmigrated through endothelium-coated transwell filters in response to control medium or indicated bone marrow-derived macrophage conditional medium (BMDM-CM). Bar = 500 μm. The quantitative data are mean ± SE of three independent experiments. *$P < 0.02$ versus control medium. (b) B16F10 cell transendothelial migrations induced by various BMDM-CM were performed in the absence or presence of indicated antibodies. Data are mean ± SE of four independent experiments. *$P < 0.02$ versus control medium; †$P < 0.05$ versus WT-CM without antibody pretreatment. (c) B16F10 cells were treated with WT or HO-1$^{+/-}$ BMDM-CM for indicated times. The levels of phospho-STAT3 and STAT3 examined by western blot analysis. (d) WT BMDM-CM pre-incubated with or without indicated antibody (1 μg/mL) for 30 min was used to treat B16F10 cells for 15 min. The levels of phospho-STAT3 and STAT3 examined by western blot analysis. CM, conditional medium.

HO activity than their counterparts (Fig. S4b). When the *in vitro* migration assay was performed, splenic WT-CD11b^{+} cells exhibited greater migration responses toward VEGF, monocyte chemoattractant protein-1 (MCP-1) and S100A8 (Fig. 5a). Nevertheless, the impaired migration response of HO-1$^{+/-}$ myeloid cells toward S100A8 could be reversed by cotreatment with a CO donor, tricarbonyldichlororuthenium (II) dimer (CORM-2), but not by the inactivated CORM-2 (Fig. 5b).[26] In parallel with the migration response, S100A8-induced transient p38 kinase phosphorylation was also much lower in HO-1$^{+/-}$ BMDM compared to WT counterparts (Fig. 5c).

Myeloid Heme oxygenase-1-induced vascular endothelial growth factor and interleukin-10 promote tumor extravasation and STAT3 signaling. The vascular permeability is crucial for tumor cell extravasation at the metastatic site. VEGF, a potent inducer of endothelial permeability, is induced by HO-1 in macrophages.[20] We confirmed the previous finding that VEGF gene expression was significantly higher in WT-BMDM than HO-1$^{+/-}$-BMDM (Fig. S5). To test whether macrophage-

derived VEGF impacts tumor cell extravasation, we performed an *in vitro* transendothelial migration assay. As shown in Figure 6(a), WT BMDM-CM induced significantly greater transendothelial migration of CMFDA-labeled B16F10 cells than HO-$1^{+/-}$ BMDM-CM. Cotreatment with VEGF neutralizing antibody, but not control IgG, resulted in the reduction of increased transendothelial migration of tumor cells induced by BMDM-CM (Fig. 6b). These observations support the involvement of HO-1-induced VEGF in macrophage-mediated tumor cell extravasation at the metastatic site.

To examine whether macrophage-derived soluble factors also contribute to the induction of survival signaling in tumor cells arrested at metastatic sites, we treated B16F10 cells with BMDM-CM for various durations and the level of STAT3 phosphorylation was determined by western blot analysis. The results showed that both WT and HO-$1^{+/-}$ BMDM-CMs induced a rapid and transient phosphorylation of STAT3 (Fig. 6c). In contrast, the level of phospho-STAT3 was much greater in cells treated with WT-BMDM-CM. Along with VEGF, WT-BMDM also expressed higher IL-10 expression comparing to HO-$1^{+/-}$ BMDM (Fig. S5). Considering that both VEGF and IL-10 are capable of inducing STAT3 phosphorylation in various cell types,[25] we tested the potential involvements of these two factors in enhanced tumor STAT3 phosphorylation induced by WT BMDM-CM. As shown in Figure 6(d), pre-treatment of WT BMDM-CM with VEGF or IL-10 neutralizing antibody, but not control IgG, significantly reduced CM-induced STAT3 phosphorylation in B16F10 cells, suggesting the involvement of macrophage-HO-1-induced VEGF and IL-10 in promoting the survival signaling of tumor cells at the early phase of metastasis.

Discussion

In the present study, we demonstrated that HO-1 has a profound effect on the prometastatic function of myeloid cells. Our data show that the migration response of $CD11b^+$ myeloid cells toward S100A8, one of the major chemoattractants implicated in the recruitment of myeloid cells to premetastatic lungs, was significantly affected by HO-1 expression via modulating S100A8-induced p38 signaling. This finding is consistent with our early report showing that HO-1 impacts the migration of macrophages to adipose tissue during obesity.[24] Moreover, the impaired migration response of HO-$1^{+/-}$ $CD11b^+$ cells could be reversed by cotreatment with a CO donor. As numerous studies have documented the role of CO in mediating various effects of HO-1,[27] our data support that HO-1/CO-modulated signaling has an impact on the recruitment of myeloid cells to form the premetastatic niche primed by tumor-derived soluble factors.

Experiments also demonstrated that significantly more monocytes/macrophages were recruited to lungs of WT mice in the early phase post-i.v. infusion of B16F10 cells. The percentage of B16F10 cells localized in the extravascular compartments was much higher in WT mice at this time point. This observation is in agreement with early reports showing that the newly recruited macrophages facilitated tumor cell extravasation, a crucial step in metastatic seeding.[9,10] It has been shown that monocyte/macrophage-derived VEGF contributes to the metastatic seeding of breast tumor in lungs.[10] Because HO-1 induces VEGF expression in macrophages, the role of myeloid HO-1-induced VEGF in modulating tumor cell extravasation was supported by the experiment showing that WT-BMDM-CM promoted greater transendothelial migration of tumor cells compared to that of HO-$1^{+/-}$ BMDM, and it could be significantly suppressed by treatment with VEGF neutralizing antibody. These findings indicate that myeloid HO-1 can impact metastatic seeding of tumor cells through VEGF induction.

Whether tumor cells can survive in the foreign microenvironments following extravasation is crucial for successful colonization and growth. Several cytokines and growth factors produced by macrophages, including HO-1-induced VEGF and IL-10, are potent activators of STAT3, a survival signal for tumor cells. When we performed phospho-STAT3 immunofluorescence staining with lung sections from WT and HO-$1^{+/-}$ mice subjected to i.v. infusion of B16F10 cells, the results showed that the positive phospho-STAT3 stain could be detected on the tumor cells retained in the lungs, and it was much more prominent in WT mice. Notably, these phospho-$STAT3^+$ tumor cells were in close proximity with macrophages, suggesting a possible relevance between macrophages and tumor STAT3 activation in the metastatic foci. This notion was further supported by the *in vitro* experiment showing that WT-BMDM-CM induced a transient STAT3 phosphorylation of B16F10 cells to a greater extent compared to HO-$1^{+/-}$ BMDM-CM. Moreover, co-treatment of WT-BMDM-CM with neutralizing antibodies against VEGF and IL-10 significantly attenuated the induction of STAT3 phosphorylation in B16F10 cells. These data support a role of HO-1 as a macrophage-mediated survival signal for metastatic tumor cells.

In sum, the present study provides the first line of evidence to demonstrate that myeloid HO-1 can facilitate tumor metastasis through promoting premetastatic niche formation and increasing tumor colonization at the metastatic site. Earlier studies have supported the crucial role of NK cells in inhibiting lung metastasis.[28–30] HO-1 has been shown to suppress NK cell-mediated cytotoxicity.[31] Therefore, the contribution of HO-1-induced NK suppression to the enhanced metastasis observed in WT mice cannot be ruled out in the present study. In any event, the design of a therapeutic strategy to specifically downregulate HO-1 expression or its activity in myeloid population may be effective for treating metastatic diseases.

Acknowledgments

This work was supported in part by funding from Academia Sinica and by a grant from the National Science Council of Taiwan (NSC 100-2320-B-001-010-MY3).

Disclosure Statement

The authors have no conflict of interest to declare.

References

1 Joyce JA, Pollard JW. Microenvironmental regulation of metastasis. *Nat Rev Cancer* 2009; **9**: 239–52.
2 Quail DF, Joyce JA. Microenvironmental regulation of tumor progression and metastasis. *Nat Med* 2013; **19**: 1423–37.
3 Ostrand-Rosenberg S, Sinha P. Myeloid-derived suppressor cells: linking inflammation and cancer. *J Immunol* 2009; **182**: 4499–506.
4 Qian BZ, Pollard JW. Macrophage diversity enhances tumor progression and metastasis. *Cell* 2010; **141**: 39–51.
5 Kaplan RN, Riba RD, Zacharoulis S *et al.* VEGFR1-positive haematopoietic bone marrow progenitors initiate the pre-metastatic niche. *Nature* 2005; **438**: 820–7.

6 Hiratsuka S, Watanabe A, Aburatani H *et al.* Tumour-mediated upregulation of chemoattractants and recruitment of myeloid cells predetermines lung metastasis. *Nat Cell Biol* 2006; **8**: 1369–75.
7 Erler JT, Bennewith KL, Cox TR *et al.* Hypoxia-induced lysyl oxidase is a critical mediator of bone marrow cell recruitment to form the premetastatic niche. *Cancer Cell* 2009; **15**: 35–44.
8 Gil-Bernabe AM, Ferjancic S, Tlalka M *et al.* Recruitment of monocytes /macrophages by tissue factor-mediated coagulation is essential for metastatic cell survival and premetastatic niche establishment in mice. *Blood* 2012; **119**: 3164–75.
9 Qian B, Deng Y, Im JH *et al.* A distinct macrophage population mediates metastatic breast cancer cell extravasation, establishment and growth. *PLoS ONE* 2009; **4**: e6562.
10 Qian BZ, Li J, Zhang H *et al.* CCL2 recruits inflammatory monocytes to facilitate breast-tumour metastasis. *Nature* 2011; **475**: 222–5.
11 Abraham NG, Kappas A. Pharmacological and clinical aspects of heme oxygenase. *Pharmacol Rev* 2008; **60**: 79–127.
12 Jozkowicz A, Was H, Dulak J. Heme oxygenase-1 in tumors: is it a false friend? *Antioxid Redox Signal* 2007; **9**: 2099–117.
13 Nishie A, Ono M, Shono T *et al.* Macrophage infiltration and heme oxygenase-1 expression correlate with angiogenesis in human gliomas. *Clin Cancer Res* 1999; **5**: 1107–13.
14 Torisu-Itakura H, Furue M, Kuwano M *et al.* Co-expression of thymidine phosphorylase and heme oxygenase-1 in macrophages in human malignant vertical growth melanomas. *Jpn J Cancer Res* 2000; **91**: 906–10.
15 Caballero F, Meiss R, Gimenez A *et al.* Immunohistochemical analysis of heme oxygenase-1 in preneoplastic and neoplastic lesions during chemical hepatocarcinogenesis. *Int J Exp Pathol* 2004; **85**: 213–22.
16 Berberat PO, Dambrauskas Z, Gulbinas A *et al.* Inhibition of heme oxygenase-1 increases responsiveness of pancreatic cancer cells to anticancer treatment. *Clin Cancer Res* 2005; **11**: 3790–8.
17 Boschetto P, Zeni E, Mazzetti L *et al.* Decreased heme-oxygenase (HO)-1 in the macrophages of non-small cell lung cancer. *Lung Cancer* 2008; **59**: 192–7.
18 Was H, Dulak J, Jozkowicz A. Heme oxygenase-1 in tumor biology and therapy. *Curr Drug Targets* 2010; **11**: 1551–70.
19 Otterbein LE, Bach FH, Alam J *et al.* Carbon monoxide has anti-inflammatory effects involving the mitogen-activated protein kinase pathway. *Nat Med* 2000; **6**: 422–8.
20 Bussolati B, Ahmed A, Pemberton H *et al.* Bifunctional role for VEGF-induced heme oxygenase-1 in vivo: induction of angiogenesis and inhibition of leukocytic infiltration. *Blood* 2004; **103**: 761–6.
21 De Wilde V, Van Rompaey N, Hill M *et al.* Endotoxin-induced myeloid-derived suppressor cells inhibit alloimmune responses via heme oxygenase-1. *Am J Transplant* 2009; **9**: 2034–47.
22 Sturge J, Todd SK, Kogianni G *et al.* Mannose receptor regulation of macrophage cell migration. *J Leukoc Biol* 2007; **82**: 585–93.
23 Huang JY, Chiang MT, Yet SF *et al.* Myeloid heme oxygenase-1 haploinsufficiency reduces high fat diet-induced insulin resistance by affecting adipose macrophage infiltration in mice. *PLoS ONE* 2012; **7**: e38626.
24 Huang JY, Chiang MT, Chau LY. Adipose overexpression of heme oxygenase-1 does not protect against high fat diet-induced insulin resistance in mice. *PLoS ONE* 2013; **8**: e55369.
25 Lee H, Pal SK, Reckamp K *et al.* STAT3: a target to enhance antitumor immune response. *Curr Top Microbiol Immunol* 2011; **344**: 41–59.
26 Motterlini R, Clark JE, Foresti R *et al.* Carbon monoxide-releasing molecules: characterization of biochemical and vascular activities. *Circ Res* 2002; **90**: E17–24.
27 Bilban M, Haschemi A, Wegiel B *et al.* Heme oxygenase and carbon monoxide initiate homeostatic signaling. *J Mol Med (Berl)* 2008; **86**: 267–79.
28 Gorelik E, Wiltrout RH, Okumura K *et al.* Role of NK cells in the control of metastatic spread and growth of tumor cells in mice. *Int J Cancer* 1982; **30**: 107–12.
29 Grundy MA, Zhang T, Sentman CL. NK cells rapidly remove B16F10 tumor cells in a perforin and interferon-gamma independent manner in vivo. *Cancer Immunol Immunother* 2007; **56**: 1153–61.
30 Takeda K, Nakayama M, Sakaki M *et al.* IFN-gamma production by lung NK cells is critical for the natural resistance to pulmonary metastasis of B16 melanoma in mice. *J Leukoc Biol* 2011; **90**: 777–85.
31 Woo J, Iyer S, Cornejo MC *et al*. Stress protein-induced immunosuppression: inhibition of cellular immune effector functions following overexpression of haem oxygenase (HSP 32). *Transpl Immunol* 1998; **6**: 84–93.

Supporting Information

Additional supporting information may be found in the online version of this article:

Data S1. Supporting materials and methods.

Fig. S1. Host heme oxygenase-1 (HO-1) expression promotes tumor metastasis from primary site.

Fig. S2. Tumor cell-conditional medium induces recruitment of myeloid-derived suppressor cells (MDSC) to lung of mice.

Fig. S3. Pulmonary gene expression induced by tumor cell-conditional medium is not affected by heme oxygenase-1 (HO-1) genotype in mice.

Fig. S4. Effect of hematopoietic heme oxygenase-1 (HO-1) haploinsufficiency on HO-1 expression and activity.

Fig. S5. Vascular endothelial growth factor (VEGF) and interleukin-10 (IL-10) expressions are up-regulated in wild type (WT) macrophages.

Table S1. The primer sets used for RT-qPCR analysis.